DOI: 10.17617/2.3217942
Proceedings of the 9th Solar Polarization Workshop SPW9
A workshop held in Göttingen, Germany, from August 26 to August 30, 2019
Achim Gandorfer, Andreas Lagg, Kerstin Raab (eds.)

Solution of Polarized Radiative Transfer Equation with Cross-redistribution

K. N. Nagendra[1,2] **and M. Sampoorna**[1]

[1]Indian Institute of Astrophysics, Koramangala, Bengaluru 560 034, India
[2]Istituto Ricerche Solari Locarno, Locarno Monti, Switzerland

Abstract. We briefly present our approximate approach to the problem of polarized line formation in multi-level atoms taking into account the effects of partial frequency redistribution (PFR) and cross-redistribution (XRD). We also present the influence of XRD on linear polarization profiles, taking the examples of Ca II H and K and IR triplet lines, and the ^{3}P–^{3}S triplets of Mg I formed in an isothermal one-dimensional atmosphere. We show that XRD produces significant effects on the linear polarization profiles when the damping widths of the line components of the multiplet are comparable, like in the case of Mg I b triplet.

1 Introduction

It is well known that realistic modeling of stellar spectra, requires going beyond the standard two-level atom model. Multi-level radiative transfer problems require simultaneous solutions of the statistical equilibrium equation (SEE) and the radiative transfer equation (RTE). In the case of complete frequency redistribution (CFR), the problem is relatively simpler because the absorption and emission profile functions are identical (see Mihalas 1978, and references therein). To solve the multi-level atom unpolarized transfer with CFR, a "complete linearization technique" was developed by Auer & Mihalas (1969), and a simpler and faster equivalent two-level atom (ETLA) approach was developed by Mihalas (1978). A very elegant multi-level accelerated lambda iteration (MALI) method was later developed by Rybicki & Hummer (1991, 1992).

In the case of partial frequency redistribution (PFR), the problem is more complex because the absorption and emission profile functions are not identical. Milkey & Mihalas (1973) developed a semi-classical "sub-level formalism" to handle multi-level atom problem with PFR. Using this formalism Milkey et al. (1975) derived the cross-redistribution (XRD) function ($R_{\rm X}$), which describes the frequency redistribution for Raman scattering on a 3-level atom. Using a quantum mechanical approach Hubeny (1982) derived the 3-level atom "generalized redistribution functions (GRFs)" ($P_{\rm I-V}$). Indeed the expressions for $R_{\rm X}$ of Milkey et al. (1975) and $P_{\rm II}$ of Hubeny (1982) are one and the same. The theory of GRFs for multi-level atoms was developed by Hubeny et al. (1983a,b, hereafter HOS theory). Based on the above, Hubeny (1985) developed an ETLA solution of RTE, using PFR function of Hummer (1962). Later, Hubeny & Lites (1995) proposed a practically elegant ETLA approach to solve the multi-level PFR radiative transfer problem. For the same transfer problem Paletou (1995) developed a MALI method including only PFR function of Hummer (1962), while

Uitenbroek (2001) developed a MALI method including GRFs.

A self-consistent theory for the problem of multi-level polarized RTE can also be formulated using the formalism of density matrix to represent both atomic polarization and polarized radiation field. SEE for the atomic density matrix elements of a multi-level atom was derived by Bommier (1977) and Bommier & Sahal-Bréchot (1978). SEE and RTE for a multi-level atom, in the density matrix formalism, was derived by Landi Degl'Innocenti (1983, 1984, 1985). The above-said density matrix formalism considers only CFR in line scattering. MALI method of Rybicki & Hummer (1991) was extended to include polarization, based on the density matrix formalism of Landi Degl'Innocenti (1983), by Trujillo Bueno (1999), Manso Sainz & Trujillo Bueno (2003), and Stepan & Trujillo Bueno (2013).

PFR scattering theories were initially developed for two-level and two-term atoms. QED theory for PFR in a two-level atom was developed by Omont et al. (1972, 1973). A tractable form of their theory for use in astrophysical line formation studies as well as numerical methods to evaluate the PFR matrices were presented in Domke & Hubeny (1988). A "master equation theory" for PFR in a two-level atom was proposed in Bommier (1997a,b). A classical oscillator theory for the same problem was developed in Bommier & Stenflo (1999). Their PFR matrix was transformed to the laboratory frame by Sampoorna et al. (2007a,b). The Kramers-Heisenberg scattering approach for scattering in two-level and two-term atoms (see Fig. 1) was presented in Stenflo (1994, 1997, 1998) for 'frequency coherent scattering', which was extended to include PFR in Sampoorna (2011), Smitha et al. (2011, 2012, 2013), and Sowmya et al. (2014a,b, 2015). In the above-cited papers the lower-level polarization was neglected, which was included in the two-level atom case in Supriya et al. (2016).

Density matrix theory to handle collisionless PFR in multi-level systems was developed by Landi Degl'Innocenti et al. (1997) using a metalevel approach . Extension of Kramers-Heisenberg approach for polarized scattering in multi-level systems was presented by Stenflo (2015, 2016). Generalization of "master equation theory" to handle collisional PFR in polarized multi-level/ multi-term systems has been developed by Bommier (2016, 2017). An alternative QED theory for the same problem has been proposed in Casini et al. (2014), Casini & Manso Sainz (2016a,b), and Casini et al. (2017a,b). An approximate approach based on HOS theory for multi-level polarized RTE with PFR has been proposed in Sampoorna et al. (2013) and Sampoorna & Nagendra (2017). Here we present a brief summary of the results presented in the above-mentioned last two papers, and discuss them under the perspective of the cross-redistribution process.

2 Formulation of the problem

We first recall the unpolarized multi-level PFR transfer problem and then present our extension of the same to include polarization. Consider an N-level model atom. The SEE for level l can be written as

$$n_l \sum_{j\neq l}(C_{lj} + R_{lj}) - \sum_{j\neq l} n_j(C_{jl} + R_{jl}) = 0, \tag{1}$$

where C_{lj} and R_{lj} are the collisional and radiative rates for the transition $l \rightarrow j$ respectively. The number densities of the levels l and j are denoted by n_l and n_j respectively. The radiative upward rates are $R_{lj} = B_{lj}\bar{J}_{lj}$ and the downward rates are $R_{jl} = A_{jl} + B_{jl}\bar{J}_{lj}$, where A and B are the Einstein's coefficients. The frequency integrated "mean intensity" of the radiation

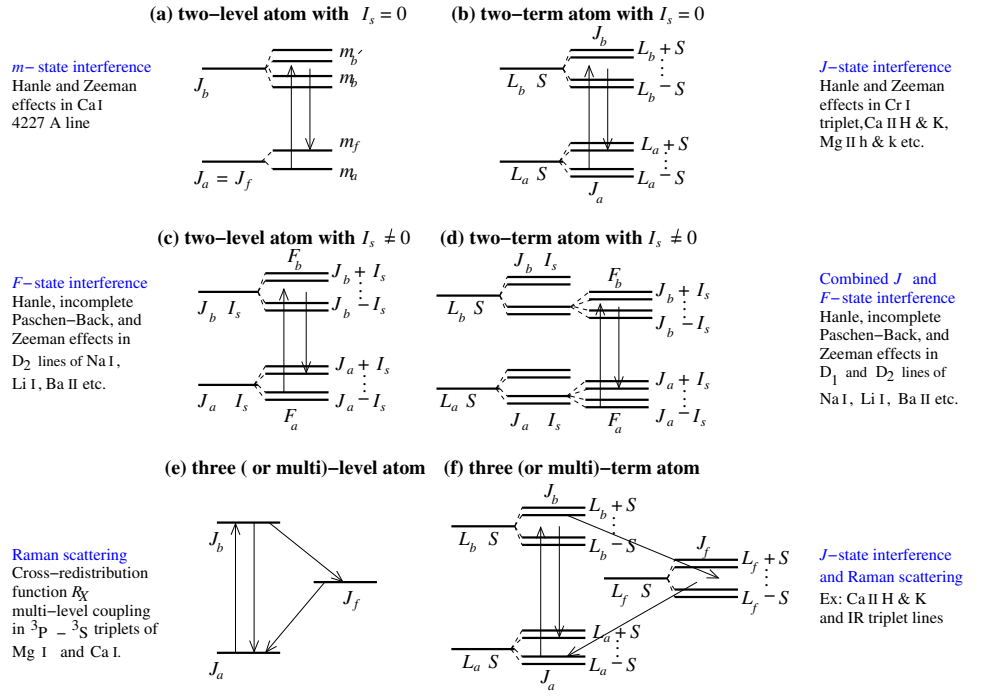

Figure 1. Level diagrams with increasing levels of complexity (a-f). Here J, L, S, and m denote the total electronic, orbital, spin, and magnetic quantum numbers respectively. Nuclear spin is denoted by I_s, and F denotes the hyperfine structure states.

field is defined as

$$\bar{J}_{lj} = \int_{-\infty}^{+\infty} J_{lj}(x)\,\varphi_{lj}(x)\,dx, \quad \text{with the mean intensity} \quad J_{lj}(x) = \int_{-1}^{+1} I_{lj}(x,\mu)\frac{d\mu}{2}\,. \tag{2}$$

In the above equations $\varphi_{lj}(x)$ is the Voigt absorption profile for $l \rightarrow j$ transition, $I_{lj}(x,\mu)$ is the specific intensity at frequency x and angle μ, where $\mu = \cos\theta$, with θ being the colatitude of the ray with respect to the atmospheric normal.

The RTE for the specific intensity $I_{lj}(x,\mu)$ in a line that arises due to a transition between an upper level j and lower level l of a multi-level atom can be written as

$$\mu[dI_{lj}(x,\mu)/dz] = -\Big[\chi_{lj}(x) + \chi_c\Big]\Big[I_{lj}(x,\mu) - S_{jl}(x)\Big], \tag{3}$$

where χ_c denotes the background continuum absorption coefficient. The total source function is given by

$$S_{jl}(x) = p_x S^L_{jl}(x) + (1-p_x) S^c_{jl}(x), \qquad \text{where} \qquad p_x = \chi_{lj}(x)/[\chi_{lj}(x) + \chi_c]. \tag{4}$$

The continuum source function is $S^c_{jl}(x) = B_{\nu_{lj}}$, with $B_{\nu_{lj}}$ being the Planck function at the line center of the transition $l \rightarrow j$. The line source function is given by $S^L_{jl}(x) = \eta_{jl}(x)/\chi_{lj}(x)$.

The line absorption coefficient is given by $\chi_{lj}(x) = [h\nu_{lj}/4\pi]\left[n_l B_{lj}\varphi_{lj}(x) - n_j B_{jl}\psi_{jl}(x)\right]$. The line emission coefficient has the form $\eta_{jl}(x) = [h\nu_{lj}/4\pi]n_j A_{jl}\psi_{jl}(x)$, where the line emission profile function is given by (see Hubeny et al. 1983a,b)

$$\psi_{jl}(x) = \frac{\varphi_{lj}(x)}{n_j P_j}\left\{\underbrace{n_l B_{lj}\bar{J}_{ljl}(x)}_{\text{Term I}} + \underbrace{\sum_{\substack{k\neq l,j\\ k<j}} n_k B_{kj}\bar{P}_{kjl}(x)}_{\text{Term II}} + \underbrace{\left[n_l C_{lj} + \sum_{k\neq l,j} n_k(A_{kj}+C_{kj})\right]}_{\text{Term III}}\right\}, \tag{5}$$

where P_j is the total rate out of level j. The Term III represents the non-scattering contribution to the line emission profile. The Term I represents the contribution of the ordinary resonance scattering process $l \rightarrow j \rightarrow l$ (i.e., absorption and re-emission in the same transition). In this term

$$\bar{J}_{ljl}(x) = \int_{-\infty}^{+\infty}[R_{ljl}(x,x')/\varphi_{lj}(x)]J_{lj}(x')dx', \tag{6}$$

$$\text{where} \qquad R_{ljl}(x,x') = \gamma_{\rm coh}R^{\rm II,AA}(x,x') + (1-\gamma_{\rm coh})R^{\rm III,AA}(x,x'). \tag{7}$$

Here $R^{\rm II,AA}$ and $R^{\rm III,AA}$ are the angle-averaged type-II and type-III PFR functions of Hummer (1962). The Term II represents the Raman scattering process $k \rightarrow j \rightarrow l$, starting from some level $k < j$. In this term

$$\bar{P}_{kjl}(x) = \int_{-\infty}^{+\infty}[P_{kjl}(x,x')/\varphi_{lj}(x)]J_{kj}(x')dx', \tag{8}$$

$$\text{where} \qquad P_{kjl}(x,x') = \gamma_{\rm coh}P^{\rm II,AA}_{kjl}(x,x') + (1-\gamma_{\rm coh})P^{\rm III,AA}_{kjl}(x,x'). \tag{9}$$

Here $P^{\rm II,AA}_{kjl}$ and $P^{\rm III,AA}_{kjl}$ are the angle-averaged type-II and type-III GRFs of Hubeny (1982). The coherence fraction $\gamma_{\rm coh} = P_j/[P_j + \Gamma_{\rm E}]$, with $\Gamma_{\rm E}$ the elastic collision rate. Thus the unpolarized line source function $S^L_{jl}(x) = \eta_{jl}(x)/\chi_{lj}(x)$ takes the form

$$S^L_{jl}(x) = \frac{A_{jl}/P_j}{n_l B_{lj} - n_j B_{jl}\rho_{jl}(x)}\left\{n_l B_{lj}\bar{J}_{ljl}(x) + \sum_{\substack{k\neq l,j\\ k<j}} n_k B_{kj}\bar{P}_{kjl}(x) + \left[n_l C_{lj} + \sum_{k\neq l,j} n_k(A_{kj}+C_{kj})\right]\right\}, \tag{10}$$

where $\rho_{jl}(x) = \psi_{jl}(x)/\varphi_{lj}(x)$. We extend Eq. (10) to include polarization. The polarized line source vector is then given by

$$\boldsymbol{S}^L_{jl}(x,\boldsymbol{\Omega}) = \frac{A_{jl}/P_j}{n_l B_{lj} - n_j B_{jl}\rho_{jl}(x)}$$
$$\times\left\{n_l B_{lj}\bar{\boldsymbol{J}}_{ljl}(x,\boldsymbol{\Omega}) + \sum_{\substack{k\neq l,j\\ k<j}} n_k B_{kj}\bar{\boldsymbol{P}}_{kjl}(x,\boldsymbol{\Omega}) + \left[n_l C_{lj} + \sum_{k\neq l,j} n_k(A_{kj}+C_{kj})\right]\boldsymbol{U}\right\}, \tag{11}$$

where $\boldsymbol{U} = [1,0,0]^{\rm T}$. Note that we have kept the quantity $\rho_{jl}(x)$ as scalar, which is equivalent to assuming that induced emission of radiation is isotropic. The polarized resonance scattering integral is given by

$$\bar{\boldsymbol{J}}_{ljl}(x,\boldsymbol{\Omega}) = \int_{-\infty}^{+\infty}\oint \frac{\mathbf{R}_{ljl}(x,\boldsymbol{\Omega},x',\boldsymbol{\Omega}',\boldsymbol{B})}{\varphi_{lj}(x)}\boldsymbol{I}_{lj}(x',\boldsymbol{\Omega}')\frac{d\Omega'}{4\pi}dx', \tag{12}$$

where $\boldsymbol{I}_{lj}(x,\boldsymbol{\Omega}) = [I_{lj}, Q_{lj}, U_{lj}]^{\rm T}$ is the 3-component Stokes vector, $\boldsymbol{\Omega}'(\theta',\phi')$ denotes the incoming ray direction about the atmospheric normal, and $d\Omega' = \sin\theta' d\theta' d\phi'$. The quantity $\mathbf{R}_{ljl}(x,\boldsymbol{\Omega},x',\boldsymbol{\Omega}',\boldsymbol{B})$ denotes the redistribution matrix for resonance scattering in a weak magnetic field $\boldsymbol{B}$ (Hanle effect) and is given in Bommier (1997b). The polarized Raman scattering integral is given by

$$\bar{\boldsymbol{P}}_{kjl}(x,\boldsymbol{\Omega}) = \int_{-\infty}^{+\infty} \oint \frac{\mathbf{R}_{kjl}(x,\boldsymbol{\Omega},x',\boldsymbol{\Omega}',\boldsymbol{B})}{\varphi_{lj}(x)} \boldsymbol{I}_{kj}(x',\boldsymbol{\Omega}') \frac{d\Omega'}{4\pi} dx' \,. \tag{13}$$

Here $\mathbf{R}_{kjl}$ denotes the Raman scattering redistribution matrix in the presence of a weak magnetic field. We assume it to be given by the same form as the resonance scattering redistribution matrix, but with $R^{\rm II,AA}$ and $R^{\rm III,AA}$ replaced by $P^{\rm II,AA}_{kjl}$ and $P^{\rm III,AA}_{kjl}$ respectively. Further the K-multipole atomic polarizability factor W_K (with $K = 0, 2$) of resonance scattering is now replaced by the corresponding factor for Raman scattering, which is given by (Stenflo 1994; Landi Degl'Innocenti & Landolfi 2004)

$$W_K(J_k,J_j,J_l) = (-1)^{J_k-J_l} 3(2J_j+1) \left\{ \begin{array}{ccc} 1 & 1 & K \\ J_j & J_j & J_k \end{array} \right\} \left\{ \begin{array}{ccc} 1 & 1 & K \\ J_j & J_j & J_l \end{array} \right\}, \tag{14}$$

where J's denote the total angular momentum quantum numbers. The Stokes vector $\boldsymbol{I}_{lj}(x,\boldsymbol{\Omega})$ satisfies the following polarized RTE

$$\mu[d\boldsymbol{I}_{lj}(x,\boldsymbol{\Omega})/dz] = -\Big[\chi_{lj}(x) + \chi_c\Big]\Big[\boldsymbol{I}_{lj}(x,\boldsymbol{\Omega}) - \boldsymbol{S}_{jl}(x,\boldsymbol{\Omega})\Big]. \tag{15}$$

The polarized total source vector is given by

$$\boldsymbol{S}_{jl}(x,\boldsymbol{\Omega}) = p_x \boldsymbol{S}^L_{jl}(x,\boldsymbol{\Omega}) + (1-p_x)\boldsymbol{S}^c_{jl}(x), \tag{16}$$

where the unpolarized continuum source vector $\boldsymbol{S}^c_{jl}(x) = B_{\nu_{ij}}\boldsymbol{U}$.

The numerical scheme to solve the polarized line transfer problem for a "multi-level system" consists of two steps. In Step I, we solve the unpolarized multi-level atom transfer problem taking into account both PFR and XRD. We basically generalize the MALI-PFR method of Paletou (1995) to include XRD. In Step 2, the number densities, line opacities $\chi_{lj}(x)$, and $\rho_{jl}(x)$ computed in Step I are kept fixed. Using these as inputs, the polarized transfer equations are solved by applying either a Polarized ALI (PALI) method (Faurobert-Scholl et al. 1997; Paletou & Faurobert-Scholl 1997; Nagendra et al. 1998, 1999; Fluri et al. 2003; Anusha & Nagendra 2011, see Nagendra 2003, 2014 for a review of PALI methods), or a Scattering Expansion Method (SEM: Frisch et al. 2009, see Nagendra 2019 for a review of SEM applied to problems of increasing complexity). For more details on our approach to polarized multilevel problems the reader is referred to Sampoorna et al. (2013). A historical account of the numerical methods for polarized RTE are presented in the review by Nagendra (2019).

3 Polarized line profiles in a five-level Ca II atom

We have applied our approximate multi-level formulation to the case of a five-level Ca II atom model comprising of the H and K lines and the IR triplet lines (see top left panel in Fig. 2).

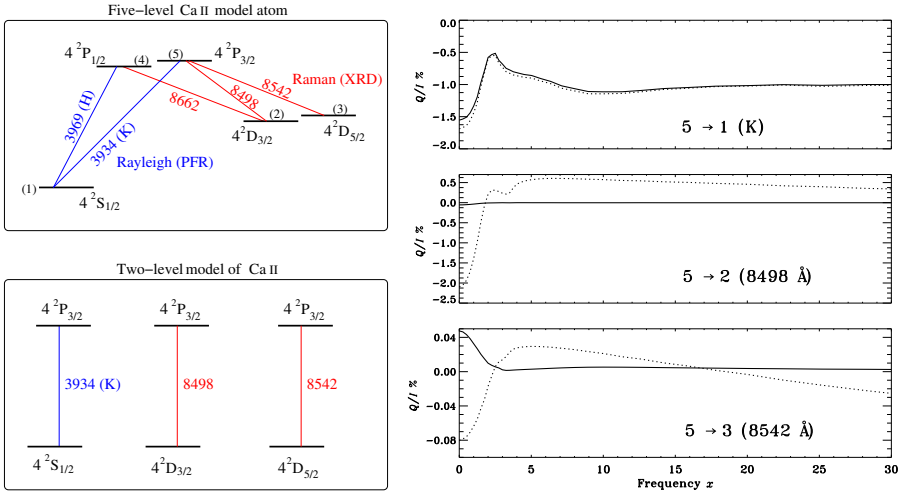

Figure 2. Top left : Five-level Ca II atom model. Bottom left : Each of the lines of five-level Ca II atom treated as resulting from two-level atom models. Right : Comparison of Q/I profiles computed using a five-level atom model (solid lines) with those computed using a two-level atom model (dotted lines). The line of sight is at $\mu = 0.047$.

The right panels of Fig. 2 show a comparison of linear polarization (Q/I) produced by five-level atom model (solid line) with that from a two-level atom model (dotted line). All the atomic and atmospheric parameters are the same as those given in Sampoorna et al. (2013). The H line and 8662 Å line show zero linear polarization as their atomic polarizability factors W_2 are 0. We note that, we do not account for lower-level polarization which is shown to be important to interpret the observed linear polarization profiles of IR triplet lines (Manso Sainz & Trujillo Bueno 2003). From Fig. 2, we see that the linear polarization of IR triplet depends on the coupling with the H and K lines. Thus, multi-level effects are important when interpreting observed polarization profiles of IR triplet lines. However PFR and XRD effects are found to be not significant in IR triplet lines, while PFR is essential to produce the Q/I profiles of K line (see Sampoorna et al. 2013, for more details). This is because IR triplet lines are subordinate lines, and also their damping widths are an order of magnitude smaller than those of resonance lines.

4 Polarized line profiles in a four-level Mg I atom

Here we consider the case of ^{3}P-^{3}S triplet of Mg I (see left panel in Fig. 3). In this case there are nine possible fluorescent transitions. Among them three are due to resonance scattering and six are due to Raman scattering. Trujillo Bueno (1999, 2001, see also Supriya et al. 2020) showed the importance of including lower-level polarization for modeling linear polarization profiles of Mg I b triplet. However, here we neglect the effects of lower-level polarization, which may be included following a numerical procedure presented in Supriya et al. (2016).

A comparison of (I, Q/I) profiles of Mg I b triplet when computed with and without Raman scattering as well as with and without CFR is shown in Fig. 3. All the atomic and

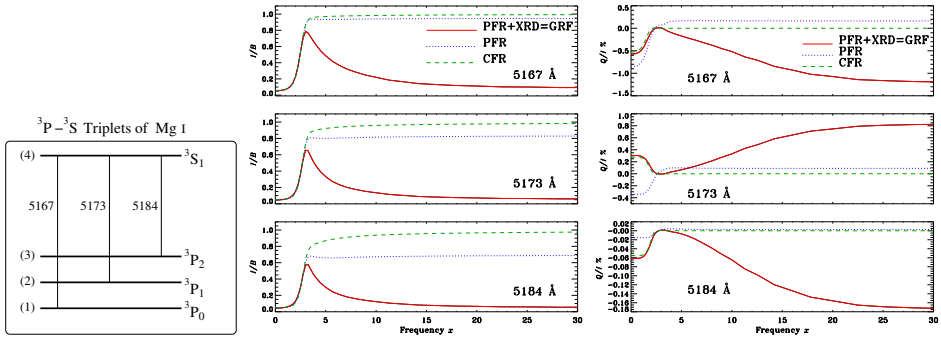

Figure 3. Left : Four-level Mg I atom model. Middle and Right : Normalized I (middle panels) and Q/I (right panels) profiles of Mg I b triplet formed in an isothermal planar atmosphere. The line of sight is at $\mu = 0.047$. Red solid lines are computed accounting for both PFR and XRD, blue dotted lines are computed taking into account only PFR, and green dashed lines are computed by assuming CFR for both resonance and Raman scattering.

atmospheric parameters are the same as those given in Sampoorna & Nagendra (2017). The red solid and green dashed lines are computed accounting for both resonance and Raman scattering contributions. While GRFs (PFR for resonance scattering and XRD for Raman scattering) is considered for red solid lines, CFR (for both resonance and Raman scattering) is assumed to compute green dashed lines. The blue dotted lines are computed neglecting the contribution from the Raman scattering, and accounting only for PFR in resonance scattering.

When XRD is included, the differences are seen in the wings of I profiles for all the three lines. Q/I profiles show a large difference between PFR without Raman scattering (blue dotted lines) and PFR with Raman scattering (red solid lines). This is because, the polarizability factors are different for resonance and Raman scattering. Q/I profiles computed with CFR (namely, all transitions in CFR: green dashed lines) and PFR+XRD (each transition in PFR/XRD: red solid lines) coincide in the line core, while they differ in the wings. Thus XRD effects are significant when the damping widths of the line components of the multiplet are comparable (see also Anusha et al. 2014, 2015).

5 Conclusions

We have developed an approximate approach to the problem of polarized line formation in a multi-level system accounting for PFR in scattering. Basically, we have extended the unpolarized PFR multi-level formulation of Hubeny et al. (1983a,b) to include scattering line polarization. We propose a two-stage approach to solve this transfer problem. We show that multi-level coupling and Raman scattering are necessary in the computation of scattering polarization in a multi-level system. We also show that XRD produces significant effects on the linear polarization profiles when the damping widths of the line components of the multiplet are comparable.

Acknowledgements. We acknowledge the use of the high-performance computing facility at Indian Institute of Astrophysics. K. N. Nagendra acknowledges the partial support by the organizers of SPW9

and also by Dr. M. Bianda, Director, IRSOL, that enabled him to participate in the workshop. He is also thankful to the Director, IIA for extending the research facilities. K. N. Nagendra presented this joint work as a contributed talk at the SPW9, and was a principal contributor to the drafting of this paper. However, he passed away unexpectedly, before submitting the paper for publication.

References

Anusha, L. S. & Nagendra, K. N. 2011, ApJ, 726, 6
Anusha, L. S., Nagendra, K. N., & Uitenbroek, H. 2014, ApJ, 794, 17
Anusha, L. S., Nagendra, K. N., & Uitenbroek, H. 2015, in Polarimetry: From the Sun to Stars and Stellar Environments, ed. K. N. Nagendra, S. Bagnulo, R. Centeno & M. J. Martínez González, IAUS 305, 234
Auer, L. H. & Mihalas, D. 1969, ApJ, 158, 641
Bommier, V. 1977, Thěse de 3eme Cycle, Paris VI Univ.
Bommier, V. 1997a, A&A, 328, 706
Bommier, V. 1997b, A&A, 328, 726
Bommier, V. 2016, A&A, 591, A59
Bommier, V. 2017, A&A, 607, A50
Bommier, V. & Sahal-Bréchot, S. 1978, A&A, 69, 57
Bommier, V. & Stenflo, J. O. 1999, A&A, 350, 327
Casini, R., Landi Degl'Innocenti, M., Manso Sainz, R., Landi Degl'Innocenti, E., & Landolfi, M. 2014, ApJ, 791, 94
Casini, R., del Pino Aleman, T., & Manso Sainz, R. 2017a, ApJ, 848, 99
Casini, R. & Manso Sainz, R. 2016a, ApJ, 824, 135
Casini, R. & Manso Sainz, R. 2016b, ApJ, 833, 197
Casini, R., Manso Sainz, R., & del Pino Aleman, T. 2017b, ApJ, 850, 162
Domke, H. & Hubeny, I. 1988, ApJ, 334, 527
Faurobert-Scholl, M., Frisch, H., & Nagendra, K. N. 1997, A&A, 322, 896
Fluri, D. M., Nagendra, K. N., & Frisch, H. 2003, A&A, 400, 303
Frisch, H., Anusha, L. S., Sampoorna, M., & Nagendra, K. N. 2009, A&A, 501, 335
Hubeny, I. 1982, JQSRT, 27, 593
Hubeny, I. 1985, Bull. Astron. Inst. Czechosl., 36, 1
Hubeny, I., & Lites, B. W. 1995, ApJ, 455, 376
Hubeny, I., Oxenius, J., & Simonneau, E. 1983a, JQSRT, 29, 477
Hubeny, I., Oxenius, J., & Simonneau, E. 1983b, JQSRT, 29, 495
Hummer, D. G. 1962, MNRAS, 125, 21
Landi Degl'Innocenti, E. 1983, Solar Physics, 85, 3
Landi Degl'Innocenti, E. 1984, Solar Physics, 91, 1
Landi Degl'Innocenti, E. 1985, Solar Physics, 102, 1
Landi Degl'Innocenti, E., Landi Degl'Innocenti, M., & Landolfi, M. 1997, in Proc. Forum THÉMIS, Science with THÉMIS, ed. N. Mein & S. Sahal-Bréchot (Paris: Obs. Paris-Meudon), 59
Landi Degl'Innocenti, E. & Landolfi, M. 2004, Polarization in spectral lines (Dordrecht: Kluwer)
Manso Sainz, R. & Trujillo Bueno, J. 2003, Physical Review Letters, 91, 111102
Mihalas, D. 1978, Stellar Atmosphere (2nd ed.; San Francisco, CA: Freeman)
Milkey, R. W. & Mihalas, D. 1973, ApJ, 185, 709
Milkey, R. W., Shine, R. A., & Mihalas, D. 1975, ApJ, 199, 718
Nagendra, K. N. 2003, in Stellar Atmosphere Modeling, ed. I. Hubeny, D. Mihalas, & K. Werner, ASP Conf. Ser. 288, 583

Nagendra, K. N. 2014, in Solar Polarization 7, ed. K. N. Nagendra, J. O. Stenflo, Zhongquan Qu, & M. Sampoorna, ASP Conf. Ser. 489, 179
Nagendra, K. N. 2019, in Radiative Signatures from the Cosmos, ed. K. Werner, C. Stehle, T. Rauch, & T. Lanz, ASP Conf. Ser. 519, 51
Nagendra, K. N., Frisch, H., & Faurobert-Scholl, M. 1998, A&A, 332, 610
Nagendra, K. N., Paletou, F., Frisch, H., & Faurobert-Scholl, M. 1999, in Solar Polarization, ed. K. N. Nagendra, & J. O. Stenflo, ASSL 243, 127
Omont, A., Smith, E. W., & Cooper, J. 1972, ApJ, 175, 185
Omont, A., Smith, E. W., & Cooper, J. 1973, ApJ, 182, 283
Paletou, F. 1995, A&A, 302, 587
Paletou, F. & Faurobert-Scholl, M. 1997, A&A, 328, 343
Rybicki, G. B. & Hummer, D. G. 1991, A&A, 245, 171
Rybicki, G. B. & Hummer, D. G. 1992, A&A, 262, 209
Sampoorna, M. 2011, ApJ, 731, 114
Sampoorna, M. & Nagendra, K. N. 2017, ApJ, 838, 95
Sampoorna, M., Nagendra, K. N., & Stenflo, J. O. 2007a, ApJ, 663, 625
Sampoorna, M., Nagendra, K. N., & Stenflo, J. O. 2007b, ApJ, 670, 1485
Sampoorna, M., Nagendra, K. N., & Stenflo, J. O. 2013, ApJ, 770, 92
Smitha, H. N., Nagendra, K. N., Sampoorna, M., & Stenflo, J. O. 2013, JQSRT, 115, 46
Smitha, H. N., Sampoorna, M., Nagendra, K. N., & Stenflo, J. O. 2011, ApJ, 733, 4
Smitha, H. N., Sowmya, K., Nagendra, K. N., Sampoorna, M., & Stenflo, J. O. 2012, ApJ, 758, 112
Sowmya, K., Nagendra, K. N., Stenflo, J. O., & Sampoorna, M. 2014a, ApJ, 786, 150
Sowmya, K., Nagendra, K. N., Sampoorna, M., & Stenflo, J. O. 2014b, ApJ, 793, 71
Sowmya, K., Nagendra, K. N., Sampoorna, M., & Stenflo, J. O. 2015, ApJ, 814, 127
Stenflo, J. O. 1994, Solar magnetic fields - Polarized radiation diagnostics (Dordrecht: Kluwer)
Stenflo, J. O. 1997, A&A, 324, 344
Stenflo, J. O. 1998, A&A, 338, 301
Stenflo, J. O. 2015, ApJ, 801, 70
Stenflo, J. O. 2016, arXiv:1610.09861
Stepan, J. & Trujillo Bueno, J. 2013, A&A, 557, A143
Supriya, H. D., Nagendra, K. N., Sampoorna, M., Stenflo, J. O., & Ravindra, B. 2020, Solar Polarization 8, ed. L. Belluzzi, J. Trujillo Bueno, R. Casini, & M. Romoli, ASP Conf. Ser., In Press
Supriya, H. D., Sampoorna, M., Nagendra, K. N., Stenflo, J. O., & Ravindra, B. 2016, ApJ, 828, 84
Trujillo Bueno, J. 1999, in Solar Polarization, ed. K. N. Nagendra & J. O. Stenflo, ASSL 243, 73
Trujillo Bueno, J. 2001, in Advanced Solar Polarimetry: Theory, Observations and Instrumentation, ed. M. Sigwarth, ASP Conf. Ser. 236, 161
Uitenbroek, H. 2001, ApJ, 557, 389